Pergamon

Int. J. Heat Mass Transfer. Vol. 38, No. 15, pp. 2779–2796, 1995

0017-9310/95 $9.50+0.00

0017-9310(95)00028-3

Local thermal equilibrium for transient heat conduction: theory and comparison with numerical experiments

MICHEL QUINTARD
L.E.P.T.-ENSAM (UA CNRS), Esplanade des Arts et Métiers, 33405 Talence cedex, France

and

STEPHEN WHITAKER
Department of Chemical Engineering and Material Science, University of California at Davis, Davis, CA 95616, U.S.A.

(*Received* 26 *March* 1994 *and in final form* 28 *December* 1994)

Abstract—Local thermal equilibrium refers to the state in which a single temperature can be used to describe a heat transfer process in a multiphase system. When this condition occurs, a one-equation model can be used and the analysis of the heat transfer process is greatly simplified. In this paper we first develop the constraints that must be satisfied in order that the principle of local thermal equilibrium be valid, and we then compare these constraints with numerical experiments for transient heat conduction in two-phase systems. Reasonable agreement between the estimates and the numerical experiments is obtained.

INTRODUCTION

The general problem of conduction and convection with heterogeneous and homogeneous thermal sources has been explored by Whitaker [1], and in this work we present a detailed study of transient heat conduction in a two-phase system. In particular we illustrate how previously neglected topological effects can be included in the analysis in a simple manner. The system under consideration is illustrated in Fig. 1 and the governing equations and boundary conditions are given by

$$(\rho c_p)_\beta \frac{\partial T_\beta}{\partial t} = \nabla \cdot (k_\beta \nabla T_\beta) \quad \text{in the } \beta\text{-phase} \tag{1}$$

B.C. 1 $$T_\beta = T_\sigma, \quad \text{at the } \beta\text{–}\sigma \text{ interface} \tag{2}$$

B.C. 2 $$-\mathbf{n}_{\beta\sigma} \cdot k_\beta \nabla T_\beta = -\mathbf{n}_{\beta\sigma} \cdot k_\sigma \nabla T_\sigma \quad \text{at the } \beta\text{–}\sigma \text{ interface} \tag{3}$$

$$(\rho c_p)_\sigma \frac{\partial T_\sigma}{\partial t} = \nabla \cdot (k_\sigma \nabla T_\sigma) \quad \text{in the } \sigma\text{–phase} \tag{4}$$

B.C. 3 $$T_\beta = \mathscr{F}(\mathbf{r}, t) \quad \text{at } \mathscr{A}_{\beta e} \tag{5}$$

B.C. 4 $$T_\sigma = \mathscr{G}(\mathbf{r}, t) \quad \text{at } \mathscr{A}_{\sigma e} \tag{6}$$

I.C.1 $$T_\beta = \mathscr{H}(\mathbf{r}) \quad t = 0 \tag{7}$$

I.C.2 $$T_\sigma = \mathscr{I}(\mathbf{r}) \quad t = 0. \tag{8}$$

The boundary conditions at $\mathscr{A}_{\beta e}$ and $\mathscr{A}_{\sigma e}$ are generally known only in terms of the average temperature and not in terms of the point temperature, thus equations (5) and (6) serve as reminders of what we *do not know* about T_β and T_σ. The same can be said of the initial conditions given by equations (7) and (8); however, there are some processes for which one might be able to specify the point temperatures at the boundary of the macroscopic system and at $t = 0$. The matter of boundary conditions at $\mathscr{A}_{\beta e}$ and $\mathscr{A}_{\sigma e}$ has been explored by Prat [2–4] and by Sahraoui and Kaviany [5], and the use of a two-equation model to analyze the heat transfer process near a solid surface has been studied by Plumb [6].

The volume averaged form of equation (1) is given by [7]

$$\varepsilon_\beta (\rho c_p)_\beta \frac{\partial \langle T_\beta \rangle^\beta}{\partial t} = \nabla \cdot \left[k_\beta \left(\varepsilon_\beta \nabla \langle T_\beta \rangle^\beta + \frac{1}{\mathscr{V}} \int_{A_{\beta\sigma}} \mathbf{n}_{\beta\sigma} T_\beta \, dA \right) \right] + \frac{1}{\mathscr{V}} \int_{A_{\beta\sigma}} \mathbf{n}_{\beta\sigma} \cdot k_\beta \nabla T_\beta \, dA \tag{9}$$

while the analogous form for the σ-phase is expressed as

$$\varepsilon_\sigma (\rho c_p)_\sigma \frac{\partial \langle T_\sigma \rangle^\sigma}{\partial t} = \nabla \cdot \left[k_\sigma \left(\varepsilon_\sigma \nabla \langle T_\sigma \rangle^\sigma + \frac{1}{\mathscr{V}} \int_{A_{\sigma\beta}} \mathbf{n}_{\sigma\beta} \tilde{T}_\sigma \, dA \right) \right] + \frac{1}{\mathscr{V}} \int_{A_{\sigma\beta}} \mathbf{n}_{\sigma\beta} \cdot k_\sigma \nabla T_\sigma \, dA. \tag{10}$$

Here the *intrinsic average temperatures* are defined by

$$\langle T_\beta \rangle^\beta = \frac{1}{\mathscr{V}} \int_{V_\beta} T_\beta \, dV \quad \langle T_\sigma \rangle^\sigma = \frac{1}{\mathscr{V}} \int_{V_\sigma} T_\sigma \, dV \tag{11}$$

NOMENCLATURE

a_v interfacial area per unit volume [m^{-1}]
$\mathscr{A}_{\beta e}$ area of the entrances and exists of the β-phase at the boundary of the macroscopic region [m^2]
$\mathscr{A}_{\sigma e}$ area of the entrances and exits of the σ-phase at the boundary of the macroscopic region [m^2]
$A_{\beta\sigma}$ $= A_{\sigma\beta}$, area of the β–σ interface contained within the macroscopic region [m^2]
$\mathbf{b}_\beta$ vector that maps $\nabla\langle T\rangle$ onto $\tilde{T}_\beta$ [m]
$(\rho c_p)_\alpha$ specific heat for the α-phase [J m^{-3} K^{-1}]
$(\rho c_p)_{\beta\sigma}$ $\varepsilon_\sigma(\rho c_p)_\beta+\varepsilon_\beta(\rho c_p)_\sigma$, mixed-mode specific heat for the β–σ system [J m^{-3} K^{-1}]
$\langle\rho\rangle C_p$ $\varepsilon_\beta(\rho c_p)_\beta+\varepsilon_\sigma(\rho c_p)_\sigma$, volume averaged heat capacity [J m^{-3} K^{-1}]
$\mathbf{C}_{\beta\sigma}$ tortuosity tensor associated with the temperature difference, $\langle T_\beta\rangle^\beta-\langle T_\sigma\rangle^\sigma$ [W m^{-1} K^{-1}]
H height of experimental system [m]
h heat transfer coefficient [W m^{-2} K^{-1}]
$\mathbf{I}$ unit tensor.
k_β thermal conductivity of the β-phase [W m^{-1} K^{-1}]
k_σ thermal conductivity of the σ-phase [W m^{-1} K^{-1}]
$k_{\beta\sigma}$ $\varepsilon_\sigma k_\beta+\varepsilon_\beta k_\sigma$, mixed-mode thermal conductivity for the β–σ system [W m^{-1} K^{-1}]
$\mathbf{K}_{eff}$ effective thermal conductivity tensor for the one-equation model [W m^{-1} K^{-1}]
l_β characteristic length scale for the β-phase [m]
l_σ characteristic length scale for the σ-phase [m]
$l_{\beta\sigma}$ $\sqrt{\varepsilon_\beta\varepsilon_\sigma k_{\beta\sigma}/a_v h}$, mixed-mode, small length scale for the β–σ system [m]
L_T characteristic length for $\nabla\langle T_\beta\rangle^\beta$, $\nabla\langle T_\sigma\rangle^\sigma$ or $\nabla\langle T\rangle$ [m]
L_{T1} characteristic length for $\nabla\nabla\langle T_\beta\rangle^\beta$, $\nabla\nabla\langle T_\sigma\rangle^\sigma$ or $\nabla\nabla\langle T\rangle$ [m]
L_o length of experimental system [m]
$\mathbf{n}_{\beta\sigma}$ $-\mathbf{n}_{\sigma\beta}$, unit normal vector directed from the β-phase toward the σ-phase
r_1 inner radius of Chang's unit cell [m]
r_2 outer radius of Chang's unit cell [m]
t time [s]
t^* characteristic process time [s]
T_α temperature of the α-phase [K]
$\tilde{T}_\alpha$ $T_\alpha-\langle T_\alpha\rangle^\alpha$, spatial deviation temperature of the α-phase [K]
$\langle T\rangle$ $\varepsilon_\beta\langle T_\beta\rangle^\beta+\varepsilon_\sigma\langle T_\sigma\rangle^\sigma$, spatial average temperature of the β–σ system [K]
$\hat{T}_\alpha$ $\langle T_\alpha\rangle^\alpha-\langle T\rangle$, large-scale spatial deviation temperature for the α-phase [K]
$\mathscr{V}$ local averaging volume [m^3]
V_α volume of the α-phase or α-region contained within the averaging volume [m^3]
X x/L_0.

Greek symbols

$\alpha_{\beta\sigma}$ $k_{\beta\sigma}/(\rho c_p)_{\beta\sigma}$, mixed-mode thermal diffusivity [m^2 s^{-1}]
ε_α volume fraction of the α-phase [$V_\alpha/\mathscr{V}$]
$\langle\Theta\rangle$ $(\langle T\rangle-T_1)/(T_2-T_1)$, dimensionless spatial average temperature
$\langle\Theta_\alpha\rangle^\alpha$ $(\langle T_\alpha\rangle^\alpha-T_1)/(T_2-T_1)$, dimensionless intrinsic average temperature for the α-phase.
ρ total mass density [kg m^{-3}]
τ $K_{eff}t/L_o^2\langle\rho\rangle C_p$, dimensionless time.

and the *spatial deviation temperatures* are identified by the following decompositions

$$T_\beta=\langle T_\beta\rangle^\beta+\tilde{T}_\beta \quad T_\sigma=\langle T_\sigma\rangle^\sigma+\tilde{T}_\sigma. \tag{12}$$

If the two intrinsic average temperatures, $\langle T_\beta\rangle^\beta$ and $\langle T_\sigma\rangle^\sigma$, are *sufficiently close* to each other, they can be replaced by the spatial average temperature which takes the form

$$\langle T\rangle=\frac{1}{\mathscr{V}}\int_{\mathscr{V}} T\,dV=\varepsilon_\beta\langle T_\beta\rangle^\beta+\varepsilon_\sigma\langle T_\sigma\rangle^\sigma. \tag{13}$$

One can then add equations (9) and (10) to provide the basis for a one-equation model in terms of the temperature, $\langle T\rangle$. The final form requires the development of a closure problem [8] so that the spatial deviation temperatures, $\tilde{T}_\beta$ and $\tilde{T}_\sigma$, can be represented in terms of the gradient of the spatial average temperature.

When $\langle T_\beta\rangle^\beta$ and $\langle T_\sigma\rangle^\sigma$ are *not sufficiently close* to each other, one must proceed to the two-equation model which is given by [9]

$$\beta\text{-phase:}\quad \varepsilon_\beta(\rho c_p)_\beta\frac{\partial\langle T_\beta\rangle^\beta}{\partial t}=\nabla\cdot(\mathbf{K}_{\beta\beta}\cdot\nabla\langle T_\beta\rangle^\beta+\mathbf{K}_{\beta\sigma}\cdot\nabla\langle T_\sigma\rangle^\sigma)-a_v h(\langle T_\beta\rangle^\beta-\langle T_\sigma\rangle^\sigma) \tag{14}$$

$$\sigma\text{-phase:}\quad \varepsilon_\sigma(\rho c_p)_\sigma\frac{\partial\langle T_\sigma\rangle^\sigma}{\partial t}=\nabla\cdot(\mathbf{K}_{\sigma\beta}\cdot\nabla\langle T_\beta\rangle^\beta+\mathbf{K}_{\sigma\sigma}\cdot\nabla\langle T_\sigma\rangle^\sigma)-a_v h(\langle T_\sigma\rangle^\sigma-\langle T_\beta\rangle^\beta). \tag{15}$$

The use of equations (14) and (15) is simplified by the following reciprocity relation;

$$\mathbf{K}_{\beta\sigma} = \mathbf{K}_{\sigma\beta} \tag{16}$$

however, determination of the four transport coefficients represents a formidable task and this provides considerable motivation for the use of a one-equation model whenever possible. Development of the two-equation model and its domain of validity is documented in [9], and higher order estimates of the macroscopic interphase heat flux have been proposed in [10].

Local gradient equilibrium

The first simplification that can be made in terms of equations (14) and (15) occurs when the gradients, $\nabla\langle T_\beta\rangle^\beta$ and $\nabla\langle T_\sigma\rangle^\sigma$, are sufficiently close so that they can be set equal to each other in the separate transport equations. We refer to this condition as *local gradient equilibrium* and it leads to a two-equation model of the form

β-phase:

$$\varepsilon_\beta(\rho c_p)_\beta \frac{\partial\langle T_\beta\rangle^\beta}{\partial t} = \nabla\cdot[(\mathbf{K}_{\beta\beta}+\mathbf{K}_{\beta\sigma})\cdot\nabla\langle T_\beta\rangle^\beta] - a_v h(\langle T_\beta\rangle^\beta - \langle T_\sigma\rangle^\sigma) \tag{17}$$

σ-phase:

$$\varepsilon_\sigma(\rho c_p)_\sigma \frac{\partial\langle T_\sigma\rangle^\sigma}{\partial t} = \nabla\cdot[(\mathbf{K}_{\sigma\beta}+\mathbf{K}_{\sigma\sigma})\cdot\nabla\langle T_\sigma\rangle^\sigma] - a_v h(\langle T_\sigma\rangle^\sigma - \langle T_\beta\rangle^\beta). \tag{18}$$

This model requires the determination of two conductivity tensors and the volumetric heat transfer coefficient, $a_v h$. The experimental determination of these three coefficients represents a challenging experimental problem, thus one is still motivated to make use of the condition of local thermal equilibrium whenever possible.

Local thermal equilibrium

When $\langle T_\beta\rangle^\beta$ and $\langle T_\sigma\rangle^\sigma$ can be set equal to the spatial average temperature defined by equation (13), one can add equations (17) and (18) to obtain the one-equation model. We express this result as

$$\langle\rho\rangle C_p \frac{\partial\langle T\rangle}{\partial t} = \nabla\cdot(\mathbf{K}_{\text{eff}}\cdot\nabla\langle T\rangle) \tag{19}$$

in which we have used the following definitions

$$\langle\rho\rangle C_p = \varepsilon_\beta(\rho c_p)_\beta + \varepsilon_\sigma(\rho c_p)_\sigma \tag{20}$$

$$\mathbf{K}_{\text{eff}} = \mathbf{K}_{\beta\beta} + 2\mathbf{K}_{\beta\sigma} + \mathbf{K}_{\sigma\sigma}. \tag{21}$$

In order to apply equation (19) with confidence, one needs to know what is meant by the phrase, $\langle T_\beta\rangle^\beta$ and $\langle T_\sigma\rangle^\sigma$ *are sufficiently close*, and in the next section we will develop constraints that provide meaning to this phrase.

LOCAL THERMAL EQUILIBRIUM

If one believes that $\langle T_\beta\rangle^\beta = \langle T_\sigma\rangle^\sigma$ is a valid *approximation*, it is prudent to propose decompositions of the form

$$\langle T_\beta\rangle^\beta = \langle T\rangle + \hat{T}_\beta, \quad \langle T_\sigma\rangle^\sigma = \langle T\rangle + \hat{T}_\sigma \tag{22}$$

and then identify the conditions for which $\hat{T}_\beta$ and $\hat{T}_\sigma$ are negligible. This requires that we substitute equations (22) into equations (9) and (10) and add the results to obtain

$$\langle\rho\rangle C_p \frac{\partial\langle T\rangle}{\partial t} = \nabla\cdot\left[(\varepsilon_\beta k_\beta + \varepsilon_\sigma k_\sigma)\nabla\langle T\rangle + \frac{k_\beta}{\mathscr{V}}\int_{A_{\beta\sigma}} \mathbf{n}_{\beta\sigma}\tilde{T}_\beta\,dA + \frac{k_\sigma}{\mathscr{V}}\int_{A_{\sigma\beta}} \mathbf{n}_{\sigma\beta}\tilde{T}_\sigma\,dA\right] - \left[\varepsilon_\beta(\rho c_p)_\beta\frac{\partial\hat{T}_\beta}{\partial t} + \varepsilon_\sigma(\rho c_p)_\sigma\frac{\partial\hat{T}_\sigma}{\partial t} - \nabla\cdot(\varepsilon_\beta k_\beta\nabla\hat{T}_\beta) - \nabla\cdot(\varepsilon_\sigma k_\sigma\nabla\hat{T}_\sigma)\right]. \tag{23}$$

When the last four terms in this volume averaged transport equation are negligible, one need only develop the closure problem for $\tilde{T}_\beta$ and $\tilde{T}_\sigma$ in order to arrive at the one-equation model given by equation (19). From the decompositions given by equations (22), we can deduce that

$$\varepsilon_\beta\hat{T}_\beta = -\varepsilon_\sigma\hat{T}_\sigma = \varepsilon_\beta\varepsilon_\sigma(\langle T_\beta\rangle^\beta - \langle T_\sigma\rangle^\sigma) \tag{24}$$

and if we are willing to ignore variations in the volume fractions, ε_β and ε_σ, we can use this result to express equation (23) as

$$\langle\rho\rangle C_p \frac{\partial\langle T\rangle}{\partial t} = \nabla\cdot\left[(\varepsilon_\beta k_\beta + \varepsilon_\sigma k_\sigma)\nabla\langle T\rangle + \frac{k_\beta}{\mathscr{V}}\int_{A_{\beta\sigma}} \mathbf{n}_{\beta\sigma}\tilde{T}_\beta\,dA + \frac{k_\sigma}{\mathscr{V}}\int_{A_{\sigma\beta}} \mathbf{n}_{\sigma\beta}\tilde{T}_\sigma\,dA\right] - \left\{\varepsilon_\beta\varepsilon_\sigma[(\rho c_p)_\beta - (\rho c_p)_\sigma]\frac{\partial}{\partial t}(\langle T_\beta\rangle^\beta - \langle T_\sigma\rangle^\sigma) - \nabla\cdot[\varepsilon_\beta\varepsilon_\sigma(k_\beta - k_\sigma)\nabla(\langle T_\beta\rangle^\beta - \langle T_\sigma\rangle^\sigma)]\right\}. \tag{25}$$

The process of discarding the last four terms in equation (25) is not a trivial matter for there is more than one way in which the Level II restrictions [11] can be arranged. Since the left hand side of equation (25) will be zero for a steady-state process, it seems wise to center our attention on the conductive terms. When local thermal equilibrium is valid we know that [12]

$$\tilde{T}_\beta = \tilde{T}_\sigma \quad \text{at the } \beta\text{–}\sigma \text{ interface} \tag{26}$$

and we also know that the spatial deviation temperature can be represented by

$$\tilde{T}_\beta = \mathbf{b}_\beta \cdot \nabla \langle T \rangle. \tag{27}$$

This allows us to approximate the conductive terms by

$$(\varepsilon_\beta k_\beta + \varepsilon_\sigma k_\sigma)\nabla\langle T\rangle + \frac{k_\beta}{\mathscr{V}}\int_{A_{\beta\sigma}} \mathbf{n}_{\beta\sigma}\tilde{T}_\beta \, dA + \frac{k_\sigma}{\mathscr{V}}\int_{A_{\sigma\beta}} \mathbf{n}_{\sigma\beta}\tilde{T}_\sigma \, dA \approx \mathbf{K}_{\text{eff}} \cdot \nabla\langle T\rangle \tag{28}$$

in which $\mathbf{K}_{\text{eff}}$ is the one-equation model effective thermal conductivity tensor defined by

$$\mathbf{K}_{\text{eff}} = (\varepsilon_\beta k_\beta + \varepsilon_\sigma k_\sigma)\mathbf{I} + \frac{(k_\beta - k_\sigma)}{\mathscr{V}}\int_{A_{\beta\sigma}} \mathbf{n}_{\beta\sigma}\mathbf{b}_\beta \, dA. \tag{29}$$

We now make use of equation (28) to simplify equation (25) by imposing the following two restrictions

$$\varepsilon_\beta\varepsilon_\sigma[(\rho c_p)_\beta - (\rho c_p)_\sigma]\frac{\partial}{\partial t}(\langle T_\beta\rangle^\beta - \langle T_\sigma\rangle^\sigma) \ll \nabla\cdot[\mathbf{K}_{\text{eff}}\cdot\nabla\langle T\rangle] \tag{30}$$

$$\nabla\cdot[\varepsilon_\beta\varepsilon_\sigma(k_\beta - k_\sigma)\nabla(\langle T_\beta\rangle^\beta - \langle T_\sigma\rangle^\sigma)] \ll \nabla\cdot[\mathbf{K}_{\text{eff}}\cdot\nabla\langle T\rangle]. \tag{31}$$

In the original analysis of this problem [1], the effective conductivity tensor in equations (30) and (31) was replaced with $(\varepsilon_\beta k_\beta + \varepsilon_\sigma k_\sigma)\mathbf{I}$; however, the approximation indicated by equation (28) certainly provides a more reliable approach since $\mathbf{K}_{\text{eff}}$ can differ greatly from $(\varepsilon_\beta k_\beta + \varepsilon_\sigma k_\sigma)\mathbf{I}$ for certain topological conditions.

To obtain useful forms of equations (30) and (31), we estimate the time and space derivatives of $\langle T_\beta\rangle^\beta$ and $\langle T_\sigma\rangle^\sigma$ according to

$$\frac{\partial}{\partial t}(\langle T_\beta\rangle^\beta - \langle T_\sigma\rangle^\sigma) = \mathbf{O}\left[\frac{\Delta(\langle T_\beta\rangle^\beta - \langle T_\sigma\rangle^\sigma)}{t^*}\right] \tag{32}$$

$$\nabla(\langle T_\beta\rangle^\beta - \langle T_\sigma\rangle^\sigma) = \mathbf{O}\left[\frac{\Delta(\langle T_\beta\rangle^\beta - \langle T_\sigma\rangle^\sigma)}{L_T}\right] \tag{33}$$

in which t^* is a characteristic process time and L_T is a characteristic length associated with changes in the volume averaged temperature. Since the temperature difference $\langle T_\beta\rangle^\beta - \langle T_\sigma\rangle^\sigma$ represents a *deviation*, as indicated by equations (22), we can approximate the change in this difference with the difference itself. This leads to the estimates

$$\frac{\partial}{\partial t}(\langle T_\beta\rangle^\beta - \langle T_\sigma\rangle^\sigma) = \mathbf{O}\left[\frac{(\langle T_\beta\rangle^\beta - \langle T_\sigma\rangle^\sigma)}{t^*}\right] \tag{34}$$

$$\nabla(\langle T_\beta\rangle^\beta - \langle T_\sigma\rangle^\sigma) = \mathbf{O}\left[\frac{(\langle T_\beta\rangle^\beta - \langle T_\sigma\rangle^\sigma)}{L_T}\right] \tag{35}$$

and the derivatives of the spatial average temperature are estimated in an analogous manner

$$\nabla\langle T\rangle = \mathbf{O}\left(\frac{\Delta\langle T\rangle}{L_T}\right) \tag{36}$$

$$\nabla\nabla\langle T\rangle = \mathbf{O}\left(\frac{\Delta\langle T\rangle}{L_{T1}L_T}\right). \tag{37}$$

Here we think of L_{T1} as the characteristic length associated with *changes in the gradient* of the volume averaged temperature, and if the gradient is constant the form of equation (37) indicates that L_{T1} is infinite. This situation occurs when the heat conduction process is steady and one-dimensional. When the estimates given by equations (34)–(37) are used in equations (30) and (31) we obtain the following two restrictions associated with the condition of local thermal equilibrium

$$\frac{\varepsilon_\beta\varepsilon_\sigma[(\rho c_p)_\beta - (\rho c_p)_\sigma]L_{T1}L_T}{\mathbf{K}_{\text{eff}}t^*}\left(\frac{\langle T_\beta\rangle^\beta - \langle T_\sigma\rangle^\sigma}{\Delta\langle T\rangle}\right) \ll 1 \tag{38}$$

$$\frac{\varepsilon_\beta\varepsilon_\sigma(k_\beta - k_\sigma)}{\mathbf{K}_{\text{eff}}}\left(\frac{\langle T_\beta\rangle^\beta - \langle T_\sigma\rangle^\sigma}{\Delta\langle T\rangle}\right) \ll 1. \tag{39}$$

For many systems of practical importance, the physical parameters and the length and time-scales will be such that

$$\frac{\varepsilon_\beta\varepsilon_\sigma[(\rho c_p)_\beta - (\rho c_p)_\sigma]L_{T1}L_T}{\mathbf{K}_{\text{eff}}t^*} \leqslant \mathbf{O}(1). \tag{40}$$

$$\frac{\varepsilon_\beta\varepsilon_\sigma(k_\beta - k_\sigma)}{\mathbf{K}_{\text{eff}}} = \mathbf{O}(1). \tag{41}$$

Under these circumstances, the condition of local thermal equilibrium will be dominated by the quantity $(\langle T_\beta\rangle^\beta - \langle T_\sigma\rangle^\sigma)/\Delta\langle T\rangle$, and it is our ability to estimate this quantity that allows us to determine when local thermal equilibrium is valid and when it is not.

ESTIMATION OF THE TEMPERATURE DIFFERENCE

The best estimate of the temperature difference, $\langle T_\beta\rangle^\beta - \langle T_\sigma\rangle^\sigma$, would be based on the governing differential equation and boundary conditions for this field. The general form of the governing equation for $\langle T_\beta\rangle^\beta - \langle T_\sigma\rangle^\sigma$ is quite complicated; however, if one ignores variations in the volume fractions, ε_β and ε_σ, one can subtract equation (10) from equation (9) to eventually obtain [1]

$$[\varepsilon_\sigma(\rho c_p)_\beta + \varepsilon_\beta(\rho c_p)_\sigma]\frac{\partial}{\partial t}(\langle T_\beta\rangle^\beta - \langle T_\sigma\rangle^\sigma) - \nabla\cdot[(\varepsilon_\sigma k_\beta + \varepsilon_\beta k_\sigma)\nabla(\langle T_\beta\rangle^\beta - \langle T_\sigma\rangle^\sigma)]$$

$$= -[(\rho c_p)_\beta - (\rho c_p)_\sigma]\frac{\partial \langle T\rangle}{\partial t} + \nabla\cdot\left[(k_\beta - k_\sigma)\nabla\langle T\rangle + \frac{k_\beta \varepsilon_\beta^{-1}}{\mathscr{V}}\int_{A_{\beta\sigma}} \mathbf{n}_{\beta\sigma}\tilde{T}_\beta \, dA - \frac{k_\sigma \varepsilon_\sigma^{-1}}{\mathscr{V}}\int_{A_{\sigma\beta}} \mathbf{n}_{\sigma\beta}\tilde{T}_\sigma \, dA\right]$$

$$+ \frac{(\varepsilon_\beta \varepsilon_\sigma)^{-1}}{\mathscr{V}}\int_{A_{\beta\sigma}} \mathbf{n}_{\beta\sigma}\cdot k_\beta \nabla T_\beta \, dA. \quad (42)$$

Here we can see the beginnings of a transport equation for $\langle T_\beta\rangle^\beta - \langle T_\sigma\rangle^\sigma$ with the accumulation and conduction terms on the left hand side, and the so-called *source terms* involving $\langle T\rangle$ on the right-hand side. In order for this result to be useful, we require that it contains only terms involving $\langle T_\beta\rangle^\beta - \langle T_\sigma\rangle^\sigma$ or $\langle T\rangle$. In the original treatment of this problem, the integrals containing $\tilde{T}_\beta$ and $\tilde{T}_\sigma$ were discarded on the basis that they are the same order of magnitude as the term $(k_\beta - k_\sigma)\nabla\langle T\rangle$. While this is usually true, these integrals contain important topological information and this is lost if these terms are discarded. A complete accounting of the integrals containing $\tilde{T}_\beta$ and $\tilde{T}_\sigma$ takes one back to the two-equation model given by equations (14) and (15); however, we can develop an approximate solution for these integrals with only a modest effort and this is done later in this paper.

On the basis of equations (26) and (27) we can express equation (42) as

$$(\rho c_p)_{\beta\sigma}\frac{\partial}{\partial t}(\langle T_\beta\rangle^\beta - \langle T_\sigma\rangle^\sigma) - \nabla\cdot[k_{\beta\sigma}\nabla(\langle T_\beta\rangle^\beta - \langle T_\sigma\rangle^\sigma)]$$

$$= -[(\rho c_p)_\beta - (\rho c_p)_\sigma]\frac{\partial\langle T\rangle}{\partial t} + \nabla\cdot\left\{\left[(k_\beta - k_\sigma)\mathbf{I} + \frac{(\varepsilon_\beta\varepsilon_\sigma)^{-1}k_{\beta\sigma}}{\mathscr{V}}\int_{A_{\beta\sigma}} \mathbf{n}_{\beta\sigma}\mathbf{b}_\beta \, dA\right]\cdot\nabla\langle T\rangle\right\}$$

$$+ \frac{(\varepsilon_\beta\varepsilon_\sigma)^{-1}}{\mathscr{V}}\int_{A_{\beta\sigma}} \mathbf{n}_{\beta\sigma}\cdot k_\beta\nabla T_\beta \, dA \quad (43)$$

in which we have introduced the mixed-mode parameters defined by

$$(\rho c_p)_{\beta\sigma} = \varepsilon_\sigma(\rho c_p)_\beta + \varepsilon_\beta(\rho c_p)_\sigma \quad k_{\beta\sigma} = \varepsilon_\sigma k_\beta + \varepsilon_\beta k_\sigma. \quad (44)$$

The interfacial heat flux can be expressed as

$$\frac{1}{\mathscr{V}}\int_{A_{\beta\sigma}} \mathbf{n}_{\beta\sigma}\cdot k_\beta\nabla T_\beta \, dA = -a_v h(\langle T_\beta\rangle^\beta - \langle T_\sigma\rangle^\sigma) \quad (45)$$

and in subsequent paragraphs we show how the heat transfer coefficient can be determined by the solution of a closure problem that is similar to the one used to determine the vector $\mathbf{b}_\beta$. In both cases we will make use of the work of Chang [13, 14] to develop analytic solutions that are comparable to those presented by Maxwell [15] and Rayleigh [16] for one-equation models of heat conduction and diffusion.

Use of equation (45) in equation (43) leads to the governing differential equation for $\langle T_\beta\rangle^\beta - \langle T_\sigma\rangle^\sigma$ given by

$$(\rho c_p)_{\beta\sigma}\frac{\partial}{\partial t}(\langle T_\beta\rangle^\beta - \langle T_\sigma\rangle^\sigma) - \nabla\cdot[k_{\beta\sigma}\nabla(\langle T_\beta\rangle^\beta - \langle T_\sigma\rangle^\sigma)] + (\varepsilon_\beta\varepsilon_\sigma)^{-1}a_v h(\langle T_\beta\rangle^\beta - \langle T_\sigma\rangle^\sigma) \quad (46)$$

$$= -[(\rho c_p)_\beta - (\rho c_p)_\sigma]\frac{\partial\langle T\rangle}{\partial t} + \nabla\cdot\left\{(k_\beta - k_\sigma)[\mathbf{I} + \mathbf{C}_{\beta\sigma}]\cdot\nabla\langle T\rangle\right\}.$$

Here the second order tensor, $\mathbf{C}_{\beta\sigma}$, is defined by

$$\mathbf{C}_{\beta\sigma} = \frac{(\varepsilon_\beta\varepsilon_\sigma)^{-1}k_{\beta\sigma}}{(k_\beta - k_\sigma)\mathscr{V}}\int_{A_{\beta\sigma}} \mathbf{n}_{\beta\sigma}\mathbf{b}_\beta \, dA \quad (47)$$

and we refer to $\mathbf{C}_{\beta\sigma}$ as the tortuosity tensor. We are assured that the right hand side of equation (46) is zero when the physical properties of the two phases are equal since the vector $\mathbf{b}_\beta$ is directly proportional to $(k_\beta - k_\sigma)$.

At this point we are ready to use equation (46) to develop an estimate of $\langle T_\beta\rangle^\beta - \langle T_\sigma\rangle^\sigma$ in terms of the characteristic change in the spatial average temperature, $\Delta\langle T\rangle$. We make use of the estimates indicated by equations (34)–(37) in order to express the left hand side of equation (46) as

$$(\rho c_p)_{\beta\sigma}\frac{\partial}{\partial t}(\langle T_\beta\rangle^\beta - \langle T_\sigma\rangle^\sigma) - \nabla\cdot[k_{\beta\sigma}\nabla(\langle T_\beta\rangle^\beta - \langle T_\sigma\rangle^\sigma)] + (\varepsilon_\beta\varepsilon_\sigma)^{-1}a_v h(\langle T_\beta\rangle^\beta - \langle T_\sigma\rangle^\sigma)$$

$$= \left\{\underbrace{\mathbf{O}\left[\frac{(\rho c_p)_{\beta\sigma}}{t^*}\right]}_{\text{accumulation}} + \underbrace{\mathbf{O}\left[\frac{k_{\beta\sigma}}{L_{T_1}L_T}\right]}_{\text{conduction}} + \underbrace{\frac{a_v h}{\varepsilon_\beta\varepsilon_\sigma}}_{\text{exchange}}\right\} \times (\langle T_\beta\rangle^\beta - \langle T_\sigma\rangle^\sigma). \quad (48)$$

Our typical estimate of the right-hand side of equation (47) is given by

$$-[(\rho c_p)_\beta - (\rho c_p)_\sigma]\frac{\partial\langle T\rangle}{\partial t} + \nabla\cdot\{(k_\beta - k_\sigma)[\mathbf{I} + \mathbf{C}_{\beta\sigma}]\cdot\nabla\langle T\rangle\}$$

$$= \left\{\mathbf{O}\left[\frac{(\rho c_p)_\beta - (\rho c_p)_\sigma}{t^*}\right] + \mathbf{O}\left[\frac{(k_\beta - k_\sigma)(1 + C_{\beta\sigma})}{L_{T_1}L_T}\right]\right\}\Delta\langle T\rangle \quad (49)$$

in which $C_{\beta\sigma}$ is some suitable norm of $\mathbf{C}_{\beta\sigma}$. In general, the estimates given by equations (34) through (37) do not take the *sign* of the individual terms into account, and this adds a degree of uncertainty to the right-hand side of equations (48) and (49) when the terms are the same order of magnitude. For equation (49) we can

develop an improved estimate on the basis of equation (19) since the one-equation model allows us to conclude that $\partial\langle T\rangle/\partial t$ and $\nabla\nabla\langle T\rangle$ have the same sign. This permits us to take the sign into account in the construction of our estimates and we do this by expressing equation (49) as

$$-[(\rho c_p)_\beta-(\rho c_p)_\sigma]\frac{\partial\langle T\rangle}{\partial t}+\nabla\cdot\{(k_\beta-k_\sigma)[\mathbf{I}+\mathbf{C}_{\beta\sigma}]\cdot\nabla\langle T\rangle\}$$
$$=\left\{\mathbf{O}\left[\frac{(\rho c_p)_\beta-(\rho c_p)_\sigma}{t^*}\right]-\mathbf{O}\left[\frac{(k_\beta-k_\sigma)(1+\mathbf{C}_{\beta\sigma})}{L_{T1}L_T}\right]\right\}\Delta\langle T\rangle \quad (50)$$

The signs of the terms on the right-hand side of equation (48) also poses a problem and we will deal with this matter later. We can now substitute equations (48) and (50) into equation (46) to obtain

$$\frac{\langle T_\beta\rangle^\beta-\langle T_\sigma\rangle^\sigma}{\Delta\langle T\rangle}=\mathbf{O}\left(\frac{l_{\beta\sigma}}{L}\right)^2$$
$$\times\left\{\frac{\mathbf{O}\left[\dfrac{((\rho c_p)_\beta-(\rho c_p)_\sigma)L^2}{k_{\beta\sigma}t^*}\right]-\mathbf{O}\left[\dfrac{(k_\beta-k_\sigma)(1+\mathbf{C}_{\beta\sigma})}{k_{\beta\sigma}}\right]}{\underbrace{1}_{\text{exchange}}+\underbrace{\mathbf{O}\left(\frac{l_{\beta\sigma}}{L}\right)^2}_{\text{conduction}}+\underbrace{\mathbf{O}\left(\frac{l_{\beta\sigma}^2}{\alpha_{\beta\sigma}t^*}\right)}_{\text{accumulation}}}\right\}. \quad (51)$$

Here we have defined the mixed-mode thermal diffusivity as

$$\alpha_{\beta\sigma}=\frac{k_{\beta\sigma}}{(\rho c_p)_{\beta\sigma}} \quad (52)$$

and the mixed-mode, small length scale is given by

$$l_{\beta\sigma}^2=\frac{\varepsilon_\beta\varepsilon_\sigma k_{\beta\sigma}}{a_v h}. \quad (53)$$

For simplicity we have replaced L_{T1} L_T with L^2, and one must remember that these two length scales will depend on time as indicated by equation (40). It is of some importance to note that L_{T1} will be *infinite* for steady, one-dimensional (1D) conduction processes, and for these conditions equation (51) indicates that $\langle T_\beta\rangle^\beta-\langle T_\sigma\rangle^\sigma$ will be zero. This means that local thermal equilibrium is always valid for steady, 1D heat conduction.

For many transient *processes*, we expect that

$$\frac{((\rho c_p)_\beta-(\rho c_p)_\sigma)L^2}{k_{\beta\sigma}t^*}=\mathbf{O}(1) \quad (54)$$

and for many *systems* of practical importance we expect that

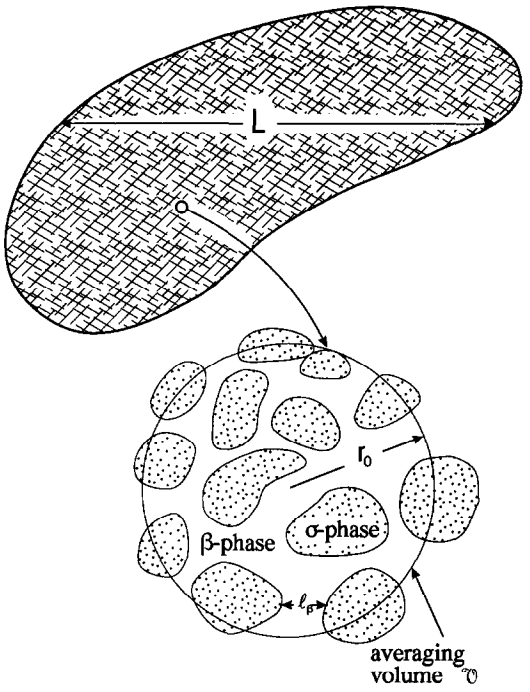

Fig. 1. Macroscopic region and averaging volume for a two-phase system.

$$\left[\frac{(k_\beta-k_\sigma)(1+\mathbf{C}_{\beta\sigma})}{k_{\beta\sigma}}\right]=\mathbf{O}(1). \quad (55)$$

Under these circumstances the term, $(l_{\beta\sigma}/L)^2$, is going to control the estimate given by equation (51) and will thus control the condition of local thermal equilibrium.

Earlier we pointed out that information about a field, such as $\langle T_\beta\rangle^\beta-\langle T_\sigma\rangle^\sigma$, was best obtained by an examination of the governing differential equation, the boundary conditions, and the initial condition. However, the estimate of $\langle T_\beta\rangle^\beta-\langle T_\sigma\rangle^\sigma$ given by equation (51) is based *only* on the governing differential equation and thus must be used with some care.

DETERMINATION OF THE TEMPERATURE DIFFERENCE

Because of the importance of equation (51), in both this study and in subsequent studies of increasing complex heat transfer processes, it is important to compare that estimate with experiments. Some laboratory values of $\langle T_\beta\rangle^\beta-\langle T_\sigma\rangle^\sigma$ are available [1–3]; however, more details can be obtained from the numerical experiments that have been carried out by Quintard and Whitaker [9] and we will use those results to test the reliability of equation (51). The numerical experiments consisted of transient, 1D (in the volume averaged sense) experiments for the nodular and stratified systems shown in Figs. 2 and 3.

Two numerical experiments were performed on the nodular system illustrated in Fig. 2 and one exper-

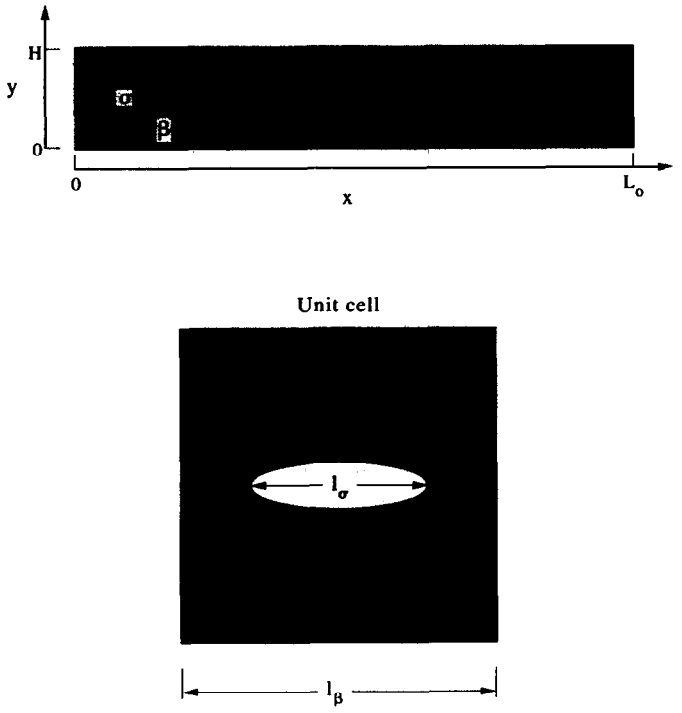

Fig. 2. Two-dimensional nodular system.

iment was performed on the stratified system illustrated in Fig. 3. These involved the solution of the boundary value problem corresponding to equations (1)–(4) and the following initial and boundary conditions

$$\text{B.C. 3} \quad T_\beta = T_2 \quad \text{at } x = 0; \quad T_\beta = T_1 \quad \text{at } x = L_0 \tag{56}$$

Nodular system

$$\text{B.C. 4} \quad \mathbf{j}\cdot\nabla T_\beta = 0 \quad \text{at } y = 0 \quad \text{and } y = H. \tag{57}$$

Stratified system

$$\text{B.C. 4}' \quad \mathbf{j}\cdot\nabla T_\sigma = 0 \quad \text{at } y = 0 \tag{58}$$

$$\text{B.C. 4}'' \quad \mathbf{j}\cdot\nabla T_\beta = 0 \quad \text{at } y = H \tag{59}$$

$$\text{I.C.} \quad T_\beta = T_\sigma = T_1 \quad \text{at } t = 0. \tag{60}$$

The numerical results were used to produce dimensionless values of the volume average temperatures defined by

$$\langle\Theta_\beta\rangle^\beta = \frac{\langle T_\beta\rangle^\beta - T_1}{T_2 - T_1} \tag{61}$$

$$\langle\Theta_\sigma\rangle^\sigma = \frac{\langle T_\sigma\rangle^\sigma - T_1}{T_2 - T_1}. \tag{62}$$

These numerical values provided profiles of $\langle\Theta_\beta\rangle^\beta$ and $\langle\Theta_\sigma\rangle^\sigma$ as functions of X and τ which are defined as

$$X = x/L_o \quad \tau = K_{\text{eff}}t/L_o^2\langle\rho\rangle C_p \tag{63}$$

and the computed profiles were compared with those obtained by solution of both the one-equation and two-equation models presented in the first part of this paper. A little thought will indicate that

$$\langle\Theta_\beta\rangle^\beta - \langle\Theta_\sigma\rangle^\sigma = \frac{\langle T_\beta\rangle^\beta - \langle T_\sigma\rangle^\sigma}{\Delta\langle T\rangle} \tag{64}$$

thus the numerical results of Quintard and Whitaker [9] can be used to test the estimate given by equation (51). To carry out that comparison, it is convenient to express equation (51) in the following dimensionless form

$$\frac{\langle T_\beta\rangle^\beta - \langle T_\sigma\rangle^\sigma}{\Delta\langle T\rangle} = \mathbf{O}\left(\frac{l_{\beta\sigma}}{L(t)}\right)^2 \times \left\{ \frac{\mathbf{O}\left[\dfrac{(\rho c_p)_\beta - (\rho c_p)_\sigma}{\langle\rho\rangle C_p}\right]\left[\dfrac{L(t)}{L_o}\right]^2\left(\dfrac{K_{\text{eff}}}{k_{\beta\sigma}}\right)\dfrac{1}{\tau} - \mathbf{O}\left[\dfrac{(k_\beta - k_\sigma)(1+\mathbf{C}_{\beta\sigma})}{k_{\beta\sigma}}\right]}{\underbrace{1}_{\text{exchange}} + \underbrace{\mathbf{O}\left(\dfrac{l_{\beta\sigma}}{L(t)}\right)^2}_{\text{conduction}}} + \underbrace{\mathbf{O}\left[\left(\dfrac{l_{\beta\sigma}}{L_o}\right)^2\left(\dfrac{K_{\text{eff}}/\langle\rho\rangle C_p}{\alpha_{\beta\sigma}\tau}\right)\right]}_{\text{accumulation}} \right\}, \tag{65}$$

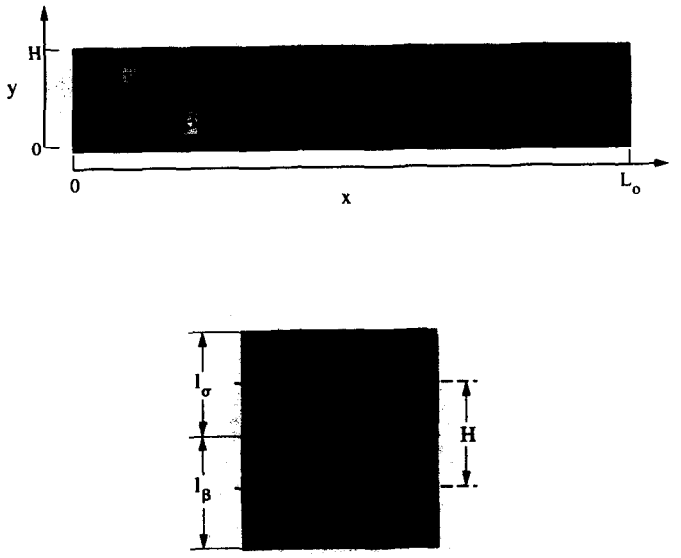

Fig. 3. Stratified system.

Here we have been careful to note that L_{T1} and L_T are functions of time, and both these macroscopic length scales have been represented by $L(t)$.

PARAMETER ESTIMATION

In order to compare equation (65) with the numerical experiments associated with the system shown in Fig. 2, we need to determine $C_{\beta\sigma}$ and the mixed-mode small length scale, $l_{\beta\sigma}$. To determine the former we recall equation (47)

$$\mathbf{C}_{\beta\sigma} = \frac{(\varepsilon_\beta \varepsilon_\sigma)^{-1} k_{\beta\sigma}}{(k_\beta - k_\sigma)\mathscr{V}} \int_{A_{\beta\sigma}} \mathbf{n}_{\beta\sigma} \mathbf{b}_\beta \, dA \tag{66}$$

and draw upon the work of Ochoa-Tapia *et al.* [17] in order to determine the vector $\mathbf{b}_\beta$ by the following closure problem

Conductivity closure problem

$$\text{B.C. 1} \qquad \mathbf{b}_\beta = 0 \quad r = r_2 \tag{67a}$$

$$\nabla^2 \mathbf{b}_\beta = 0 \quad r_1 < r \leqslant r_2 \tag{67b}$$

$$\text{B.C. 2} \qquad \mathbf{b}_\beta = \mathbf{b}_\sigma \quad r = r_1 \tag{67c}$$

$$\text{B.C. 3} \qquad -\mathbf{n}_{\beta\sigma} \cdot k_\beta \nabla \mathbf{b}_\beta = -\mathbf{n}_{\beta\sigma} \cdot k_\sigma \nabla \mathbf{b}_\sigma + \mathbf{n}_{\beta\sigma}(k_\beta - k_\sigma) \quad r = r_1 \tag{67d}$$

$$\nabla^2 \mathbf{b}_\sigma = 0 \quad 0 \leqslant r < r_1. \tag{67e}$$

This closure problem is associated with the unit cell illustrated in Fig. 4, and it was Chang [13, 14] who first showed that the solution led to Maxwell's [15] result for a 3D array of spheres and Rayleigh's [16] result for a 2D array of cylinders. Since the array of cylinders (Fig. 1) is transversely isotropic, the solution

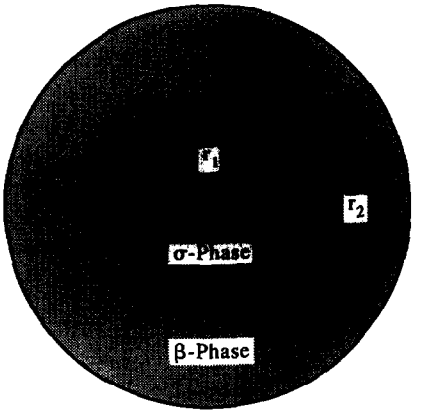

Fig. 4. Chang's unit cell.

of equations (67) leads to

$$\mathbf{i} \cdot \left\{ \frac{1}{\mathscr{V}} \int_{A_{\beta\sigma}} \mathbf{n}_{\beta\sigma} \mathbf{b}_\beta \, dA \right\} \cdot \mathbf{i} = -\frac{\varepsilon_\beta \varepsilon_\sigma (k_\beta - k_\sigma)}{2k_\beta - \varepsilon_\beta (k_\beta - k_\sigma)} \tag{68}$$

and when this result is used with equation (66) we obtain

$$1 + \mathbf{i} \cdot \mathbf{C}_{\beta\sigma} \cdot \mathbf{i} = \left(\frac{k_\beta}{k_\beta + k_{\beta\sigma}} \right). \tag{69}$$

If $k_\beta \gg k_\sigma$, the result produced by equation (69) is much different than the result for $k_\sigma \gg k_\beta$ and this difference can only be captured by retaining the integrals involving $\tilde{T}_\beta$ and $\tilde{T}_\sigma$ in equation (42).

In order to determine the heat transfer coefficient, and therefore $l_{\beta\sigma}$ as defined by equation (53), we make use of the closure problem developed by Quintard and Whitaker [9] along with Chang's unit cell. This leads to

Heat transfer coefficient closure problem

$$k_\beta \nabla^2 s_\beta = \varepsilon_\beta^{-1} a_v h \quad r_1 \leqslant r \leqslant r_2 \tag{70a}$$

$$\text{B.C. 2} \quad s_\beta = s_\sigma + 1 \quad r = r_1 \tag{70b}$$

$$\text{B.C. 3} \quad \mathbf{n}_{\beta\sigma} \cdot k_\beta \nabla s_\beta = \mathbf{n}_{\beta\sigma} \cdot k_\sigma \nabla s_\sigma \quad r = r_1 \tag{70c}$$

$$k_\sigma \nabla^2 s_\sigma = -\varepsilon_\sigma^{-1} a_v h \quad 0 \leqslant r \leqslant r_1. \tag{70d}$$

To complete the problem statement for the s_β and s_σ-fields, we require that s_β and s_σ be continuous, and we impose the condition of radial symmetry on s_β and s_σ, i.e.

$$s_\beta = s_\beta(r) \quad s_\sigma = s_\sigma(r). \tag{70e}$$

This latter condition replaces the condition of periodicity that one uses with spatially periodic models.

If $a_v h$ were known, the boundary value problem given by equations (70) would determine s_β and s_σ to within a single arbitrary constant. Both this arbitrary constant and $a_v h$ can be determined by imposing the following constraints on the s_β and s_σ-fields

$$\langle s_\beta \rangle^\beta = 0 \quad \langle s_\sigma \rangle^\sigma = 0. \tag{71}$$

The details concerning this type of analysis are given by Quintard and Whitaker [9] and here we simply note that the dimensionless form of the heat transfer coefficient for a *cylindrical system* is given by

$$\frac{a_v h r_2^2}{k_\beta} = \frac{8\varepsilon_\beta^2}{[\varepsilon_\sigma(R+1)-3]\varepsilon_\beta - 4\ln(\sqrt{(\varepsilon_\sigma)})} \tag{72}$$

in which the parameter R is defined as

$$R = \frac{\varepsilon_\beta k_\beta}{\varepsilon_\sigma k_\sigma}. \tag{73}$$

In order to develop a correspondence with the spatially periodic model shown in Fig. 2 and Chang's unit cell, we require that the volume fraction and the area per unit volume be equal, i.e.

$$\varepsilon_\beta|_{\text{Chang}} = \varepsilon_\beta \quad a_v|_{\text{Chang}} = a_v. \tag{74}$$

This leads to the following relation between r_2 and l_β

$$\pi r_2^2 = l_\beta^2 \tag{75}$$

and we have illustrated this relation in Fig. 5 where we have superimposed Chang's unit cell on the unit cell for a spatially periodic system. When equation (75) is used with equation (74) we obtain the following representation for the dimensionless heat transfer coefficient

$$\frac{a_v h l_\beta^2}{k_\beta} = \frac{8\pi\varepsilon_\beta^2}{[\varepsilon_\sigma(R+1)-3]\varepsilon_\beta - 4\ln(\sqrt{(\varepsilon_\sigma)})}$$

array of cylinders. (76)

This result is crucial for our estimation of the mixed-mode, small length-scale defined by equation (53). For the purpose of comparing theory with laboratory experiments, the solution of the spherical version of equations (70) is useful and it is given by

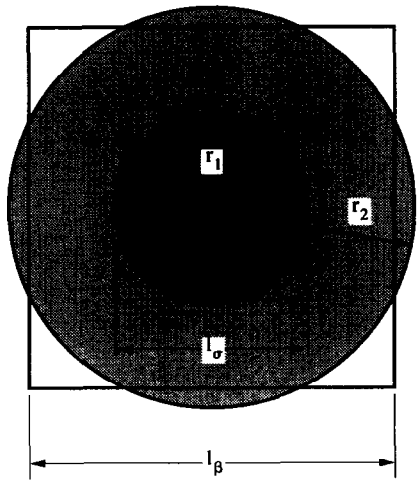

Fig. 5. Comparison of Chang's unit cell with a spatially periodic model.

$$\frac{a_v h l_\beta^2}{k_\beta} = \frac{40\alpha(\alpha^2+\alpha+1)\kappa}{(1+5\kappa)+\alpha(2+\kappa)+(\alpha^4+2\alpha^3+3\alpha^2)(1-\kappa)}$$

array of spheres. (77)

Here we have employed the following nomenclature

$$\alpha = (1-\varepsilon_\beta)^{1/3} \quad \kappa = k_\sigma/k_\beta \tag{78}$$

in order to simplify the expression for the dimensionless heat transfer coefficient.

It is of some interest to compare the solution for Chang's unit cell with the results obtained by Quintard and Whitaker [9] for a spatially periodic system, and the comparison for a wide range of conductivity ratios is presented in Figs. 6(a) and (b) for cubic arrays of both cylinders and spheres. For the arrays of cylinders (2D), we see good agreement between the analytical solution for Chang's unit cell and the numerical solution for the spatially periodic model. For the arrays of spheres (3D), the agreement is less attractive. At low values of the conductivity ratio, the 3D results are in good agreement, while at high values of this ratio Chang's unit cell predicts significantly higher values than the spatially periodic model. One should be careful to note that the logarithmic scale used in Figs. 6 tends to hide the differences between the two theoretical results, and in Fig. 7 we have shown a more detailed comparison for the 2D results. There we see significant differences at the lower values of the porosity, and this is to be expected.

While the comparison between Chang's unit cell and the spatially periodic model is attractive, it does not represent a comparison between theory and *laboratory experiments*. The single reliable experimental measurement of the heat transfer coefficient for conductive transport, of which we are aware, is found in the work of Grangeot [18]. A brief description of the Grangeot's studies of heat transfer in hexagonally packed beds of spheres is available in Grangeot *et al.* [19].

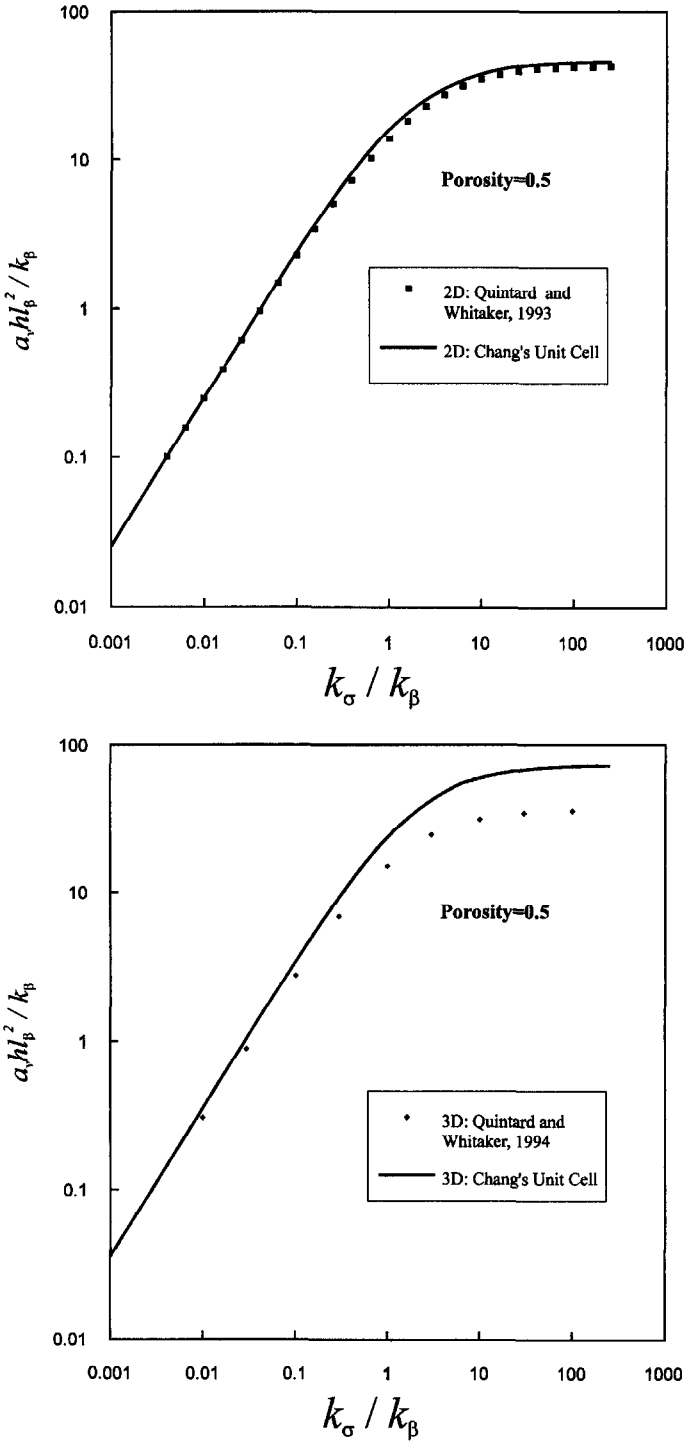

Fig. 6. (a) Dimensionless heat transfer coefficient as a function of ratio of conductivities for a periodic array of cylinders. (b) Dimensionless heat transfer coefficient as a function of ratio of conductivities for a periodic array of spheres.

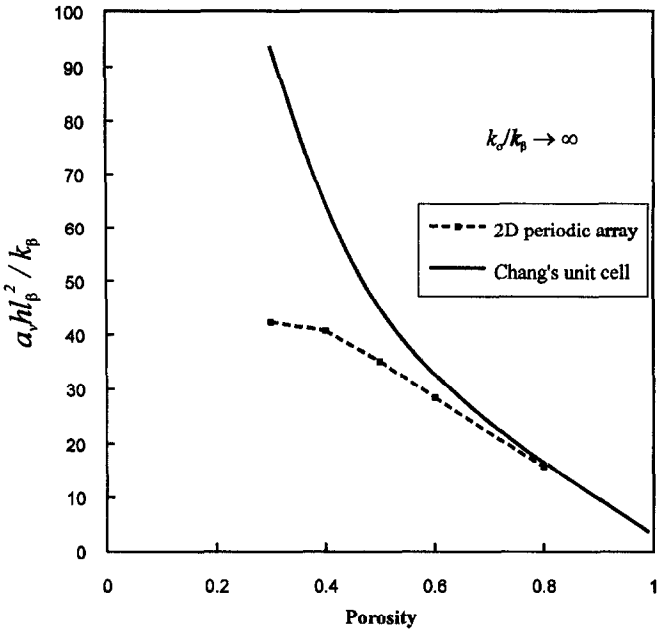

Fig. 7. Dimensionless heat transfer coefficient as a function of the porosity.

Given the parameters for the nylon-water system studied by Grangeot [18]

$$\frac{k_\sigma}{k_\beta} = 0.46 \quad \varepsilon_\beta = 0.396$$

we can use equation (77) to find

$$\left.\frac{a_v h l_\beta^2}{k_\beta}\right|_{\text{theory}} = 13.3 \quad \text{Chang's unit cell.} \tag{79}$$

This is in reasonably good agreement with the 3D spatially periodic model [19] result given by

$$\left.\frac{a_v h l_\beta^2}{k_\beta}\right|_{\text{theory}} = 11.2 \quad \text{spatially periodic model} \tag{80}$$

and both these results are in reasonable agreement with the experimental value for hexagonally packed nylon spheres and water [19].

$$\left.\frac{a_v h l_\beta^2}{k_\beta}\right|_{\text{exp}} \approx 8. \tag{81}$$

At this point we are reasonably confident that we can determine the parameters that appear in equation (65) and we are ready to compare the theory with numerical experiments.

COMPARISON WITH NUMERICAL EXPERIMENTS

Numerical experiment No. 1

Two numerical experiments were carried out for the system shown in Fig. 2, and the parameters for the first experiment are listed in Table 1. These parameters are consistent with a system composed of glass beads and air except for the porosity of the β-phase which should be on the order of 0.35–0.40. The macroscopic properties have been calculated both by the solution of a spatially periodic closure problem [9] and by the use of Chang's unit cell. The quantity $\langle\rho\rangle C_p$ is calculated directly by equation (20).

In Fig. 8 we have shown temperature profiles at dimensionless times of 0.0038 and 0.0345. In thinking about these results, one should remember that the time has been scaled so that τ will be on the order of one when steady state is reached. We express this idea as

$$\tau = \mathbf{O}(1) \quad \text{at steady state} \tag{82}$$

to make it clear that the comparisons shown in Fig. 8 are for relatively short times. The solid lines in Fig. 8 represent values of the spatial average temperature determined by equation (19), and the dimensionless temperature is defined by

$$\langle\Theta\rangle = \frac{\langle T\rangle - T_1}{T_2 - T_1}. \tag{83}$$

The values obtained directly from the numerical experiments are shown by the interrupted lines in Fig. 8, and the values of $\langle\Theta_\beta\rangle^\beta$ and $\langle\Theta_\sigma\rangle^\sigma$ were determined by equations (61) and (62) and the solution of the boundary value problem given by equations (6) through (4) and (56)–(60). For both times indicated in Fig. 8, the numerical experiments indicate that

$$\langle\Theta_\beta\rangle^\beta \approx \langle\Theta_\sigma\rangle^\sigma \approx \langle\Theta\rangle. \tag{84}$$

The experimental values begin at $X = 0.05$ since this

Table 1. Parameters for experiment No. 1 (array of cylinders)

Unit cell		ε_β 0.62	l_β/L_0 0.10	
Physical properties	k_β [W m^{-1} K^{-1}] 0.26	k_σ [W m^{-1}K^{-1}] 0.50	$(\rho c_p)_\beta$ [J m^{-3} K^{-1}] 1202	$(\rho c_p)_\sigma$ [J m^{-3} K^{-1}] 1.7×10^6
Macroscopic properties	K_{eff}/k_β	$\langle\rho\rangle C_p$ [Jm^{-3}K^{-1}]	$a_v h l_\beta^2/k_\beta$	$+C_{\beta\sigma}$
Spatially periodic	2.11	0.646×10^6	25.8	
Chang's unit cell	2.04	0.646×10^6	29.0	0.032

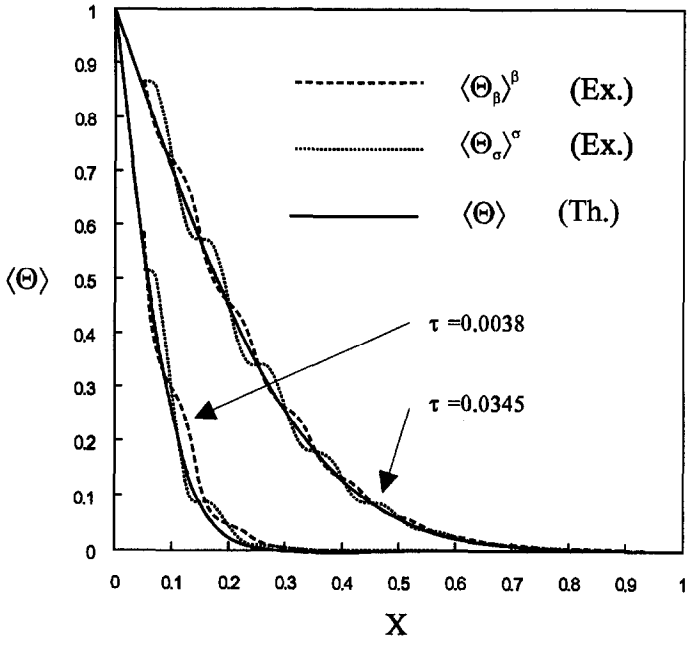

Fig. 8. Comparison of numerical experiments with the one-equation model (experiment No. 1 of Quintard and Whitaker).

represents the centroid of the first cell in the series, and the values of $\langle\Theta_\beta\rangle^\beta$ and $\langle\Theta_\sigma\rangle^\sigma$ contain small-scale fluctuations. This characteristic of volume averaged quantities has been investigated in detail by Quintard and Whitaker [20–24] who demonstrated that a double, or *cellular average*, should be used in the analysis of spatially periodic systems. If the experimental results shown in Fig. 8 were averaged a second time, it is clear that the difference between the one-equation model and the numerical experiments would be negligible. We could describe the results shown in Fig. 8 by the inequality

$$\langle\Theta_\beta\rangle^\beta - \langle\Theta_\sigma\rangle^\sigma = \frac{\langle T_\beta\rangle^\beta - \langle T_\sigma\rangle^\sigma}{\Delta\langle T\rangle} \ll 1 \qquad (85)$$

and we are now ready to examine equation (65) to see how well our estimate compares with the experimental results.

For the shortest time illustrated in Fig. 8, we have,

$$L(t) \sim 2l_\beta \qquad (86)$$

and when this result is used in equation (66) we find

$$\frac{\langle T_\beta\rangle^\beta - \langle T_\sigma\rangle^\sigma}{\Delta\langle T\rangle} = \mathbf{O}\left(\frac{l_{\beta\sigma}}{L(t)}\right)^2 \left\{\frac{\mathbf{O}(5)-\mathbf{O}(0.05)}{1+\mathbf{O}(0.025)+\mathbf{O}(0.07))}\right\}. \qquad (87)$$

At this point we should remember the discussion in which we indicated that the *signs* of the two terms in the numerator of the right-hand side of equation (65) are known (one relative to the other). This allows us to subtract 0.05 from 5; however, in this particular case this will not change our estimate of the temperature difference. The physics associated with the terms in the denominator of equation (87) are identified in equation (65), and a little thought will indicate that it is generally more difficult to determine the sign of these terms. In this particular case there is a single dominant term and that allows us to write equation (87) as

$$\frac{\langle T_\beta\rangle^\beta - \langle T_\sigma\rangle^\sigma}{\Delta\langle T\rangle} = \mathbf{O}\left(\frac{l_{\beta\sigma}}{L(t)}\right)^2 \{\mathbf{O}(5)\}. \qquad (88)$$

We have already determined that $(l_{\beta\sigma}/L(t))^2 \approx 0.025$ and we can express equation (88) as

$$\frac{\langle T_\beta\rangle^\beta - \langle T_\sigma\rangle^\sigma}{\Delta\langle T\rangle} = \mathbf{O}(0.1) \quad \tau = 0.0038 \quad \text{theory.} \tag{89}$$

In this case equation (65) clearly *over-estimates* the temperature difference since the numerical experiments would lead us to conclude that

$$\frac{\langle T_\beta\rangle^\beta - \langle T_\sigma\rangle^\sigma}{\Delta\langle T\rangle} \ll 1 \quad \tau = 0.0038 \quad \text{experiment.} \tag{90}$$

The reason behind the difference between equations (89) and (90) might well be the failure of equation (65) to take into account the influence of the initial condition which would require that

$$\frac{\langle T_\beta\rangle^\beta - \langle T_\sigma\rangle^\sigma}{\Delta\langle T\rangle} = 0 \quad \tau = 0. \tag{91}$$

Turning our attention to the second set of profiles in Fig. 8, we make use of

$$L(t) \sim 6l_\beta \quad \tau = 0.0345 \tag{92}$$

so that equation (65) provides

$$\frac{\langle T_\beta\rangle^\beta - \langle T_\sigma\rangle^\sigma}{\Delta\langle T\rangle} = \mathbf{O}\left(\frac{l_{\beta\sigma}}{L(t)}\right)^2 \left\{\frac{\mathbf{O}(5) - \mathbf{O}(0.05)}{1 + \mathbf{O}(0.003) + \mathbf{O}(0.008)}\right\}. \tag{93}$$

Clearly this leads us to

$$\frac{\langle T_\beta\rangle^\beta - \langle T_\sigma\rangle^\sigma}{\Delta\langle T\rangle} = \mathbf{O}\left(\frac{l_{\beta\sigma}}{L(t)}\right)^2 \{\mathbf{O}(5)\} \tag{94}$$

and since the ratio of length scales is given by $(l_{\beta\sigma}/L(t))^2 \approx 0.003$, we arrive at an estimate which *seems* to be in reasonable agreement with the experimental results indicated in Fig. 8.

$$\frac{\langle T_\beta\rangle^\beta - \langle T_\sigma\rangle^\sigma}{\Delta\langle T\rangle} = \mathbf{O}(0.015) \quad \tau = 0.0345 \quad \text{theory.} \tag{95}$$

One could argue that this estimate is also too large by a factor of ten or more; however, at this point it hardly matters since the use of this estimate in equations (38) and (39) will lead us to conclude that the condition of local thermal equilibrium is satisfied and that is exactly the conclusion that one would reach on the basis of the results shown in Fig. 8.

Numerical experiment No. 2

The parameters for the second numerical experiment associated with the nodular system shown in Fig. 2 are listed in Table 2. In this case the heat capacities for the two phases are equal and the thermal conductivities differ by a factor of 100. The results for two times are shown in Fig. 9 where the numerical experiments are compared with the *two-equation model* given by equations (17) and (18). The temperature profiles clearly indicate that local thermal equilibrium is *not established* for the times shown in Fig. 9 and the numerical experiments support the validity of the two-equation model.

For the temperature profile associated with the shortest time illustrated in Fig. 9, we have

$$L(t) \sim 2l_\beta \tag{96}$$

and equation (65) provides the following estimate

$$\frac{\langle T_\beta\rangle^\beta - \langle T_\sigma\rangle^\sigma}{\Delta\langle T\rangle} = \mathbf{O}\left(\frac{l_{\beta\sigma}}{L(t)}\right)^2 \left\{\frac{\mathbf{O}(1.8)}{1 + \mathbf{O}(0.1) + \mathbf{O}(1)}\right\}. \tag{97}$$

In this case we are confronted with terms in the denominator that are the same order of magnitude, and the sign of these terms now becomes crucial. In this particular case, one can refer to equations (45) and (46), and the numerical results shown in Fig. 9, to deduce that the *accumulation and interfacial flux terms are of opposite sign*. To be clear about this, we note that the accumulation and exchange terms are constrained in the following manner

$$(\rho c_p)_{\beta\sigma} \frac{\partial}{\partial t}(\langle T_\beta\rangle^\beta - \langle T_\sigma\rangle^\sigma) < 0$$

$$\text{and} \quad (\varepsilon_\beta \varepsilon_\sigma)^{-1} a_v h(\langle T_\beta\rangle^\beta - \langle T_\sigma\rangle^\sigma) > 0. \tag{98}$$

This means that equation (98) takes the form

$$\frac{\langle T_\beta\rangle^\beta - \langle T_\sigma\rangle^\sigma}{\Delta\langle T\rangle} = \mathbf{O}\left(\frac{l_{\beta\sigma}}{L(t)}\right)^2 \{\mathbf{O}(18)\} \tag{99}$$

and we estimate the temperature difference as

$$\frac{\langle T_\beta\rangle^\beta - \langle T_\sigma\rangle^\sigma}{\Delta\langle T\rangle} = \mathbf{O}(1.8) \quad \tau = 0.00437 \quad \text{theory.} \tag{100}$$

This estimate is too large by about a factor of 10 since the results shown in Fig. 9 suggest that

$$\frac{\langle T_\beta\rangle^\beta - \langle T_\sigma\rangle^\sigma}{\Delta\langle T\rangle} = \mathbf{O}(0.2) \quad \tau = 0.00437 \quad \text{experiment.} \tag{101}$$

Even though we can deduce the sign of the dominant terms in the denominator on the right hand side of equation (97), we cannot expect to obtain reasonable estimates when we are forced to use the difference between two terms that are the same order of magnitude. In order to be very clear about this point, we note that we have used $1 + \mathbf{O}(0.1) - \mathbf{O}(1) = \mathbf{O}(0.1)$ with equation (97) in order to arrive at the result given by equation (100).

Table 2. Parameters for experiment No. 2 (array of cylinders)

Unit cell		ε_β 0.62	l_β/L_0 0.10	
Physical properties	k_β [W m^{-1}K^{-1}] 1.0	k_σ [W m^{-1}K^{-1}] 0.01	$(\rho c_p)_\beta$ [J m^{-3} K^{-1}] 1.0×10^6	$(\rho c_p)_\sigma$ [J m^{-3} K^{-1}] 1.0×10^6
Macroscopic properties	K_{eff}/k_β	$\langle\rho\rangle C_p$ [Jm^{-3} K^{-1}]	$a_v h l_\beta^2/k_\beta$	$+C_{\beta\sigma}$
Spatially periodic	0.437	1.0×10^6	0.25	
Chang's unit cell	2.04	1.0×10^6	0.25	0.72

For the second set of profiles shown in Fig. 9, we have

$$L(t) \sim 4l_\beta \tag{102}$$

and equation (65) provides the estimate

$$\frac{\langle T_\beta\rangle^\beta - \langle T_\sigma\rangle^\sigma}{\Delta\langle T\rangle} = \mathbf{O}\left(\frac{l_{\beta\sigma}}{L(t)}\right)^2 \left\{\frac{\mathbf{O}(1.8)}{1+\mathbf{O}(0.02)+\mathbf{O}(0.3)}\right\}. \tag{103}$$

Once again we can argue that the accumulation and exchange terms identified in equation (65) are of opposite signs and under these circumstances equation (103) reduces to

$$\frac{\langle T_\beta\rangle^\beta - \langle T_\sigma\rangle^\sigma}{\Delta\langle T\rangle} = \mathbf{O}\left(\frac{l_{\beta\sigma}}{L(t)}\right)^2 \{\mathbf{O}(2.6)\}. \tag{104}$$

In this case the theory provides

$$\frac{\langle T_\beta\rangle^\beta - \langle T_\sigma\rangle^\sigma}{\Delta\langle T\rangle} = \mathbf{O}(0.05) \quad \tau = 0.0131 \quad \text{theory} \tag{105}$$

while the experiments indicate that

$$\frac{\langle T_\beta\rangle^\beta - \langle T_\sigma\rangle^\sigma}{\Delta\langle T\rangle} = \mathbf{O}(0.10) \quad \tau = 0.0131 \quad \text{experiment.} \tag{106}$$

Here we find that the estimate is within a factor of two of the experimental result and in general one could not expect to do better than this.

Numerical experiment No. 3

The third numerical experiment was carried out using the stratified system illustrated in Fig. 3 and the parameters for that system are given in Table 3. In this case the effective thermal conductivity refers to the component parallel to the stratification, and the dimensionless heat transfer coefficient is determined analytically in terms of the appropriate closure problem [25, 26]. The result is given by

$$\frac{a_v h(l_\beta + l_\sigma)^2}{k_\beta} = \frac{12k_\sigma}{k_{\beta\sigma}}. \tag{107}$$

It should be noted that the numerical experiments were performed on one-half of a unit cell in order to take advantage of the planes of symmetry and this means that the distance H is related to the characteristic lengths for the β and σ-phases by

$$2H = l_\beta + l_\sigma \quad \text{stratified system.} \tag{108}$$

For the particular case under consideration, i.e. $\varepsilon_\beta = \varepsilon_\sigma$, we have

$$H = l_\beta = l_\sigma. \tag{109}$$

Two sets of temperature profiles for the stratified system are shown in Fig. 10 where the numerical experiments are compared with the two-equation model. Here we see that local thermal equilibrium is not established even at relatively long times. For the smallest time illustrated in Fig. 10, we have

$$L(t) \sim 4l_\beta \tag{110}$$

and from equation (65) we have the estimate

$$\frac{\langle T_\beta\rangle^\beta - \langle T_\sigma\rangle^\sigma}{\Delta\langle T\rangle} = \left(\frac{l_{\beta\sigma}}{L(t)}\right)^2 \left\{\frac{\mathbf{O}(2)}{1+\mathbf{O}(0.13)+\mathbf{O}(1.4)}\right\}. \tag{111}$$

In this case, the numerical result shown in Fig. 10 indicate that the accumulation and interfacial flux terms are again of opposite sign

$$(\rho c_p)_{\beta\sigma}\frac{\partial}{\partial t}(\langle T_\beta\rangle^\beta - \langle T_\sigma\rangle^\sigma) > 0$$

$$\text{and} \quad (\varepsilon_\beta\varepsilon_\sigma)^{-1} a_v h(\langle T_\beta\rangle^\beta - \langle T_\sigma\rangle^\sigma) < 0. \tag{112}$$

This allows us to write

$$1+\mathbf{O}(0.13)+\mathbf{O}(1.4) = 1-\mathbf{O}(1.4) \approx \mathbf{O}(0.4) \tag{113}$$

so that equation (111) takes the form

$$\frac{\langle T_\beta\rangle^\beta - \langle T_\sigma\rangle^\sigma}{\Delta\langle T\rangle} = \left(\frac{l_{\beta\sigma}}{L(t)}\right)^2 \{\mathbf{O}(5)\}. \tag{114}$$

One must be aware that the calculation indicated by equation (113) contains all the uncertainties associated with the estimate of the transient term that provided $\mathbf{O}(1.4)$; however, it we are willing to use equations (113) and (114) we obtain the estimate

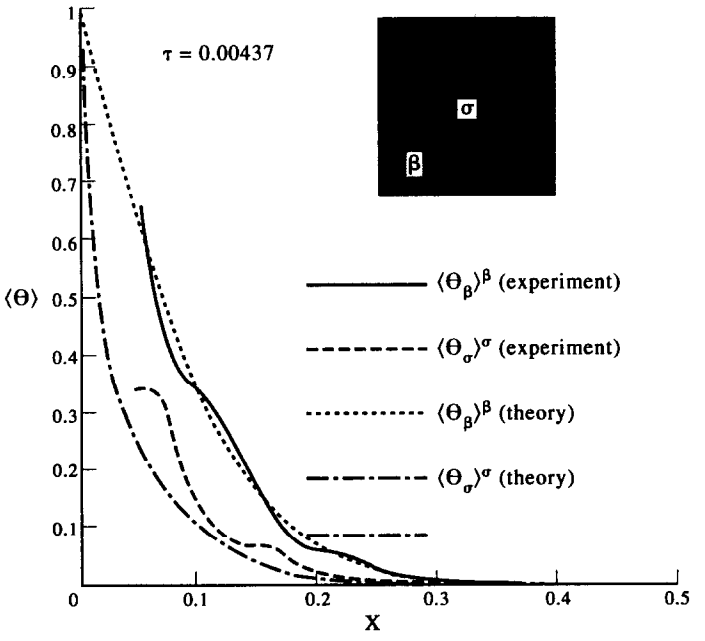

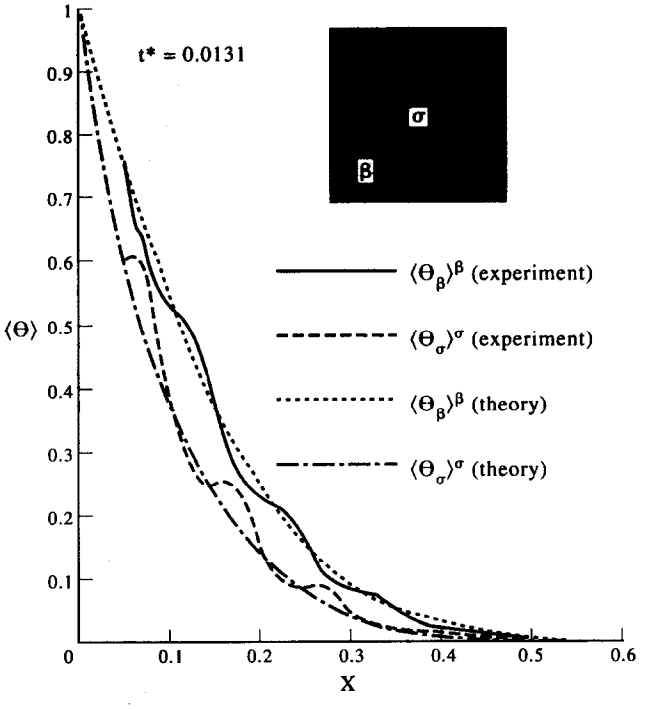

Fig. 9. Comparison of numerical experiments with the two-equation model (experiment No. 2 of Quintard and Whitaker).

$$\frac{\langle T_\beta\rangle^\beta - \langle T_\sigma\rangle^\sigma}{\Delta\langle T\rangle} = \mathbf{O}(0.6) \qquad \tau = 0.0152 \quad \text{theory.} \qquad (115)$$

$$\frac{\langle T_\beta\rangle^\beta - \langle T_\sigma\rangle^\sigma}{\Delta\langle T\rangle} = \mathbf{O}(0.3) \qquad \tau = 0.0152 \quad \text{experiment.} \qquad (116)$$

In this case our estimate of the temperature difference is larger than that indicated by the results shown in Fig. 10 which can be expressed as

For the largest time illustrated in Fig. 10, we have

$$L(t) \sim 9l_\beta \qquad (117)$$

Table 3. Parameters for experiment No. 3 (stratified system)

Unit cell		ε_β 0.50	H/L_0 0.10	
Physical properties	k_β [W m^{-1}K^{-1}] 1.0	k_σ [W m^{-1}K^{-1}] 100	$(\rho c_p)_\beta$ [J m^{-3}K^{-1}] 1.7×10^6	$(\rho c_p)_\sigma$ [J m^{-3}K^{-1}] 1.7×10^6
Macroscopic properties	K_{eff}/k_β 50.5	$\langle\rho\rangle C_p$ [Jm^{-3}K^{-1}] 1.7×10^6	$a_v H l_\beta^2/k_\beta$ 5.94	$+C_{\beta\sigma}$ 1.0

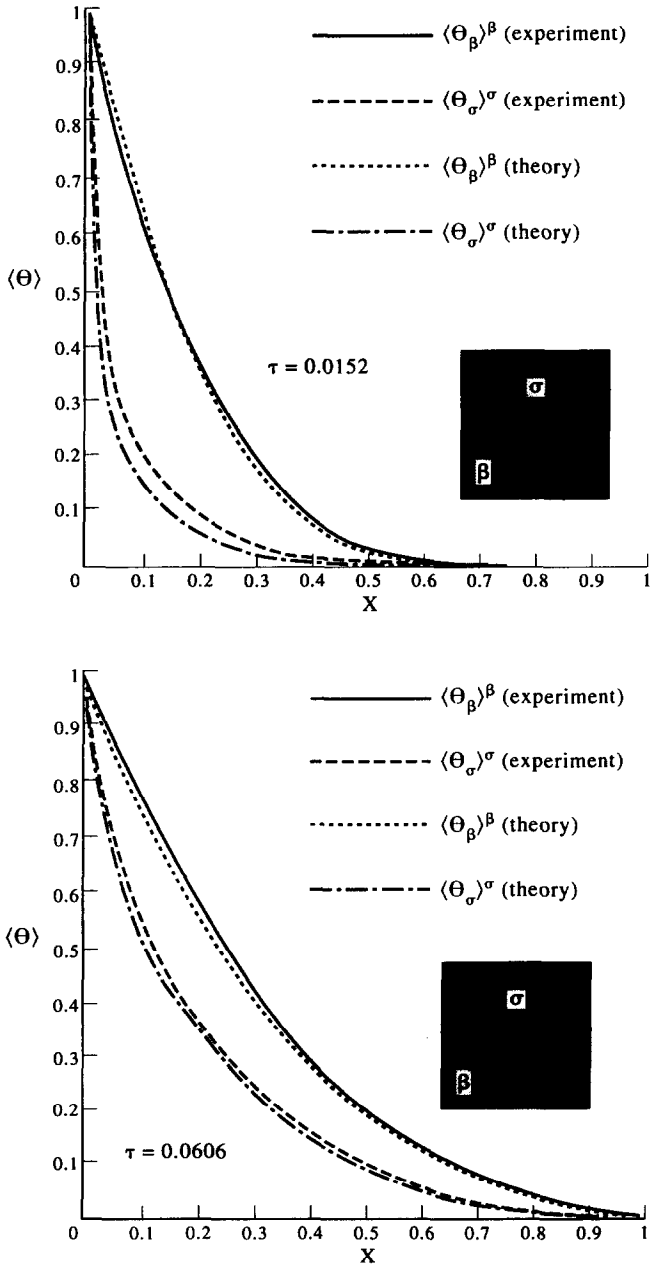

Fig. 10. Comparison of numerical experiments with the two-equation model (experiment No. 3 of Quintard and Whitaker).

and equation (65) provides

$$\frac{\langle T_\beta\rangle^\beta-\langle T_\sigma\rangle^\sigma}{\Delta\langle T\rangle}=\left(\frac{l_{\beta\sigma}}{L(t)}\right)^2\left\{\frac{\mathbf{O}(2)}{1+\mathbf{O}(0.026)+\mathbf{O}(0.35)}\right\}. \tag{118}$$

We again make use of the fact that the sign of the accumulation and exchange terms are known in order to express this result as

$$\frac{\langle T_\beta\rangle^\beta-\langle T_\sigma\rangle^\sigma}{\Delta\langle T\rangle}=\left(\frac{l_{\beta\sigma}}{L(t)}\right)^2\{\mathbf{O}(3)\} \tag{119}$$

and this leads to the theoretical result given by

$$\frac{\langle T_\beta\rangle^\beta-\langle T_\sigma\rangle^\sigma}{\Delta\langle T\rangle}=\mathbf{O}(0.08)$$

$$\tau=0.0606 \quad \text{theory.} \tag{120}$$

This provides very attractive agreement with the experimental value

$$\frac{\langle T_\beta\rangle^\beta-\langle T_\sigma\rangle^\sigma}{\Delta\langle T\rangle}=\mathbf{O}(0.1)$$

$$\tau=0.0606 \quad \text{experiment} \tag{121}$$

however, one must remember that there is considerable uncertainty in the use of order of magnitude estimates to obtain

$$1+\mathbf{O}(0.026)+\mathbf{O}(0.35)=1-\mathbf{O}(0.35)=\mathbf{O}(0.65). \tag{122}$$

For example, an estimate that indicates something is $\mathbf{O}(0.35)$ can certainly be interpreted to mean that the quantity under consideration could be as small as 0.035 or as large as 3.5.

In this test of the estimate given by equation (65) for the systems illustrated in Figs. 2 and 3, we have had some degree of success; however, much of this was based on the fact that we knew the signs of the dominant terms in the transport equation for $\langle T_\beta\rangle^\beta-\langle T_\sigma\rangle^\sigma$. In more complex applications involving multi-dimensional transport with homogeneous and heterogeneous thermal sources, it will be difficult to associate signs with the estimates of the various terms that appear in the transport equation for the temperature difference.

CONCLUSIONS

In this paper we have developed the two constraints that must be satisfied in order for local thermal equilibrium to be valid for a transient heat conduction process in a two-phase system. The current analysis represents an improvement over prior studies in that the topological effects associated both with the conductive transport terms and the heat transfer coefficient have been taken into account in terms of solutions of simple closure problems.

The analysis rests largely upon reliable estimates of the temperature difference between the two phases, and in this paper we have compared a method of estimating the temperature difference with numerical experiments for nodular and stratified systems. For several cases, in which there are significant differences in the physical properties, the estimate takes the form

$$\frac{\langle T_\beta\rangle^\beta-\langle T_\sigma\rangle^\sigma}{\Delta\langle T\rangle}=\left(\frac{l_{\beta\sigma}}{L(t)}\right)^2\{\mathbf{O}(1-10)\}. \tag{123}$$

This means that accurate determination of the mixed-mode, small length scale, $l_{\beta\sigma}$, is required in order to predict when local thermal equilibrium will occur. The uncertainty in $l_{\beta\sigma}$ is dominated by the heat transfer coefficient, h, and we have presented a convenient analytical representation for this quantity. The analytical representation is in reasonably good agreement with values obtained from spatially periodic models of porous media, and with the single experimental value that is currently available. Predicted values of the temperature difference, $\langle T_\beta\rangle^\beta-\langle T_\sigma\rangle^\sigma$, are in reasonable agreement with experimental values except when terms in the transport equation for $\langle T_\beta\rangle^\beta-\langle T_\sigma\rangle^\sigma$ are the same order of magnitude and are of opposite sign.

Acknowledgements—This work was performed while SW was a visitor at the Laboratoire Energétique et Phénomène de Transfert, and parts of the analysis were suggested during a course on transport in porous media taught in the Chemical Engineering Department at Eindhoven University of Technology. Both sources of support are greatly appreciated.

REFERENCES

1. S. Whitaker, Improved constraints for the principle of local thermal equilibrium, *Ind. Engng Chem.* **30,** 983–997 (1991).
2. M. Prat, On the boundary conditions at the macroscopic level, *Transport in Porous Media* **4,** 259–280 (1989).
3. M. Prat, Modelling of heat transfer by conduction in a transition region between a porous medium and an external fluid, *Transport in Porous Media* **5,** 71–95 (1990).
4. M. Prat, Some refinements concerning the boundary conditions at the macroscopic level, *Transport in Porous Media* **7,** 147–161 (1992).
5. M. Sahraoui and M. Kaviany, Slip and no-slip temperature boundary conditions at the interface of porous, plain media : conduction, *Int. J. Heat Mass Transfer* **36,** 1019–1033 (1993).
6. O. A. Plumb, Analysis of near wall heat transfer in porous media using a two-equation model, paper PP28, 10th International Heat Transfer Conference, Brighton, U. K. (1994).
7. M. Kaviany, *Principles of Heat Transfer in Porous Media.* Springer, New York (1991).
8. I. Nozad, R. G. Carbonell and S. Whitaker, Heat conduction in multiphase systems—I. Theory and experiment for two-phase systems, *Chem. Engng Sci.* **40,** 843–855 (1985).
9. M. Quintard and S. Whitaker, One and two-equation models for transient diffusion processes in two-phase systems. In *Adv. Heat Transfer* **23,** 369–465. Academic Press, New York (1993).
10. J. L. Auriault and P. Royer, Double conductivity media : a comparison between phenomenological and homogenization approaches, *Int. J. Heat Mass Transfer* **36,** 2613–2621 (1993).

11. S. Whitaker, Levels of simplification: the use of assumptions, restrictions and constraints in engineering analysis, *Chem. Engng Educ.* **22,** 104–108 (1988).
12. R. G. Carbonell and S. Whitaker, Heat and mass transfer in porous media. In *Fundamentals of Transport Phenomena in Porous Media* (Edited by J. Bear and M. Y. Corapcioglu), pp. 123–198. Martinus Nijhoff, Dordrecht, The Netherlands (1984).
13. H-C. Chang, Multiscale analysis of effective transport in periodic heterogeneous media, *Chem. Engng Commun.* **15,** 83–91 (1982).
14. H-C. Chang, Effective diffusion and conduction in two-phase media: a unified approach, *A.I.Ch.E.Jl.* **29,** 846–853 (1983).
15. J. C. Maxwell, *Treatise on Electricity and Magnetism* (2nd Edn) Vol. 1. Clarendon Press, Oxford (1881).
16. R. S. Rayleigh, On the influence of obstacles arranged in rectangular order upon the properties of the medium, *Phil. Mag.* **34,** 481–489 (1892).
17. J. A. Ochoa-Tapia, P. Stroeve and S. Whitaker, Diffusive transport in two-phase media: spatially periodic models and Maxwell's theory for isotropic and anisotropic systems, *Chem. Engng Sci.* **49,** 709–726 (1994).
18. G. Grangeot, Description des transferts de chaleur en milieu poreux, Thèse de Doctorat d'Etat, Université de Bordeaux I (1988).
19. G. Grangeot, M. Quintard and S. Whitaker, Heat transfer in packed beds: interpretation of experiments in terms of one- and two-equation models, *Proceedings of the 10th International Heat Transfer Conference*, Brighton, U.K., Vol. 5, pp. 291–296 (1994).
20. M. Quintard and S. Whitaker, Transport in ordered and disordered porous media—I. The cellular average and the use of weighting functions, *Transport in Porous Media* **14,** 163–177 (1994).
21. M. Quintard and S. Whitaker, Transport in ordered and disordered porous media—II. Generalized volume averaging, *Transport in Porous Media* **14,** 179–206 (1994).
22. M. Quintard and S. Whitaker, Transport in ordered and disordered porous media—III. Closure and comparison between theory and experiment, *Transport in Porous Media* **15,** 31–49 (1994).
23. M. Quintard and S. Whitaker, Transport in ordered and disordered porous media—IV. Computer generated porous media, *Transport in Porous Media* **15,** 51–70 (1994).
24. M. Quintard and S. Whitaker, Transport in ordered and disordered porous media—V. Geometrical results for two-dimensional systems, *Transport in Porous Media* **15,** 183–196 (1994).
25. J. Levec and R. G. Carbonell, Longitudinal and lateral thermal dispersion in packed beds—I. Theory, *A.I.Ch.E. Jl.* **31,** 581–590 (1985).
26. J. Levec and R. G. Carbonell, Longitudinal and lateral thermal dispersion in packed beds II: Comparison between theory and experiments, *A.I.Ch.E. Jl* **31,** 591–602 (1985).